



Dark Gravity confronted with Supernovae, Baryonic Oscillations and the Cosmic Microwave Background

Frederic Henry-Couannier

► To cite this version:

Frederic Henry-Couannier. Dark Gravity confronted with Supernovae, Baryonic Oscillations and the Cosmic Microwave Background. Seventeenth Marcel Grossmann meeting, Jul 2024, Pescara, Italy. ⟨hal-04945567⟩

HAL Id: hal-04945567

<https://hal.science/hal-04945567v1>

Submitted on 13 Feb 2025

HAL is a multi-disciplinary open access archive for the deposit and dissemination of scientific research documents, whether they are published or not. The documents may come from teaching and research institutions in France or abroad, or from public or private research centers.

L'archive ouverte pluridisciplinaire **HAL**, est destinée au dépôt et à la diffusion de documents scientifiques de niveau recherche, publiés ou non, émanant des établissements d'enseignement et de recherche français ou étrangers, des laboratoires publics ou privés.



HAL Authorization

Dark Gravity confronted with Supernovae, Baryonic Oscillations and the Cosmic Microwave Background

Frederic Henry-Couannier, Centre de Physique des Particules de Marseille, Aix-Marseille University
163 Avenue De Luminy, 13009 Marseille, France
fhenryco@yahoo.fr

Dark Gravity is a natural extension of general relativity in presence of a flat non dynamical background. Matter and radiation fields from its dark sector, as soon as their gravity dominates over our side fields gravity, produce a constant acceleration law of the scale factor. After a brief reminder of the Dark Gravity theory foundations the confrontation with the main cosmological probes is carried out. We show that, amazingly, the sudden transition between the usual matter dominated decelerated expansion law $a(t) \propto t^{2/3}$ and this accelerated expansion law $a(t) \propto t^2$ predicted by the theory should be able to fit the main cosmological probes (SN,BAO, CMB and age of the oldest stars data) but also direct H_0 measurements with two free parameters only : H_0 and the transition redshift.

1. Introduction

Dark Gravity (DG) (see the regularly updated living review in [1]) is a background dependent extension of General Relativity with an anti-gravitational sector. DG follows from a crucial observation: in the presence of a flat non dynamical background $\eta_{\mu\nu}$, it turns out that the usual gravitational field $g_{\mu\nu}$ has a twin, the "inverse" metric $\tilde{g}_{\mu\nu}$. The two being linked by:

$$\tilde{g}_{\mu\nu} = \eta_{\mu\rho}\eta_{\nu\sigma} [g^{-1}]^{\rho\sigma} = [\eta^{\mu\rho}\eta^{\nu\sigma}g_{\rho\sigma}]^{-1} \quad (1)$$

are just the two faces of a single field (no new degrees of freedom) that we called a Janus field.

The action treating our two faces of the Janus field on the same footing is achieved by simply adding to the usual action, the similar action with $\tilde{g}_{\mu\nu}$ in place of $g_{\mu\nu}$ everywhere.

$$\int d^4x (\sqrt{g}R + \sqrt{\tilde{g}}\tilde{R}) + \int d^4x (\sqrt{g}L + \sqrt{\tilde{g}}\tilde{L}) \quad (2)$$

where R and \tilde{R} are the familiar Ricci scalars respectively built from $g_{\mu\nu}$ and $\tilde{g}_{\mu\nu}$ as usual and L and \tilde{L} the Lagrangians for respectively SM F type fields propagating along $g_{\mu\nu}$ geodesics and \tilde{F} fields propagating along $\tilde{g}_{\mu\nu}$ geodesics. This theory symmetrizing the roles of $g_{\mu\nu}$ and $\tilde{g}_{\mu\nu}$ is Dark Gravity (DG) and the field equation satisfied by the Janus field derived from the minimization of the action is:

$$\begin{aligned} \sqrt{g}\eta^{\mu\sigma}g_{\sigma\rho}G^{\rho\nu} - \sqrt{\tilde{g}}\eta^{\nu\sigma}\tilde{g}_{\sigma\rho}\tilde{G}^{\rho\mu} = \\ -8\pi G(\sqrt{g}\eta^{\mu\sigma}g_{\sigma\rho}T^{\rho\nu} - \sqrt{\tilde{g}}\eta^{\nu\sigma}\tilde{g}_{\sigma\rho}\tilde{T}^{\rho\mu}) \end{aligned} \quad (3)$$

with $T^{\mu\nu}$ and $\tilde{T}^{\mu\nu}$ the energy momentum tensors for F and \tilde{F} fields respectively and $G^{\mu\nu}$ and $\tilde{G}^{\mu\nu}$ the Einstein tensors (e.g. $G^{\mu\nu} = R^{\mu\nu} - 1/2g^{\mu\nu}R$).

The minus signs in the field equation imply that we have a ghost interaction between the gravitational field and matter fields yet the classical stability about the FRW background is simple to establish. The Janus field should therefore be treated as a classical field: the theory is then free of quantum instabilities and the semi-classical path is also more natural for DG than GR as the similarity between the gravitational field and other fields is broken by the presence of $\eta^{\mu\nu}$ (see our discussion in the section 16.6 of [1]) and the fundamental discrete symmetries at the heart of the theory. See also [12] and [13] for an example of specific construction of a quantum-classical interaction.

2. The homogeneous and isotropic case

We found that an homogeneous and isotropic solution is necessarily spatially flat because the two sides of the Janus field about our flat Minkowski background are required to be both homogeneous and isotropic. The conjugate homogeneous and isotropic spatially flat metrics then take the form $g_{\mu\nu} = a(t)\eta_{\mu\nu}$ and $\tilde{g}_{\mu\nu} = \tilde{a}^{-1}(t)\eta_{\mu\nu}$. In this section the time variable t is the conformal time and the Hubble parameters H and \tilde{H} are understood to be conformal Hubble parameters. Then the two Friedman type equations the conformal scale factor should satisfy are:

$$a^2(2\dot{H} + H^2) - \tilde{a}^2(2\dot{\tilde{H}} + \tilde{H}^2) = -6K(a^4 p - \tilde{a}^4 \tilde{p}) \quad (4)$$

$$a^2 H^2 - \tilde{a}^2 \tilde{H}^2 = 2K(a^4 \rho - \tilde{a}^4 \tilde{\rho}) \quad (5)$$

with $K = \frac{4\pi G}{3}$. The second equation has the very important property that it is trivially satisfied ($0=0$) at initial time $t=0$ defined such that $a(0) = \tilde{a}(0)$ at which conjugate densities and pressures are also the same. So we are free to choose any initial condition on H (we are also free to freeze then any degree of freedom that would make the metric depart from the conformal form). But then the system has no solution except that of an empty static universe. However, let's allow the conjugate variations of the offshell gravitational constants inside both matter-radiation actions. We then have the following conservation violation equations :

$$\dot{\rho} = \Gamma\rho - 3H(\rho + p) \quad (6)$$

$$\dot{\tilde{\rho}} = \tilde{\Gamma}\tilde{\rho} - 3\tilde{H}(\tilde{\rho} + \tilde{p}) \quad (7)$$

with the "energy creation/annihilation" rates $\Gamma = \frac{\dot{G}}{G}$ and $\tilde{\Gamma} = \frac{\dot{\tilde{G}}}{\tilde{G}}$ related through $\tilde{\Gamma} = -\Gamma$ (just as $\tilde{H} = -H$). Now replacing these terms in the time derivative of the second DG-Friedman equation and then adding and subtracting the two DG-Friedman equations we get :

$$a\ddot{a} = K(a^4(\rho - 3p) + \frac{1}{2}(C_r + \tilde{C}_r)) \quad (8)$$

$$\tilde{a}\ddot{\tilde{a}} = K(\tilde{a}^4(\tilde{\rho} - 3\tilde{p}) + \frac{1}{2}(C_r + \tilde{C}_r)) \quad (9)$$

including the energy creation/annihilation terms $C_r = a^4 \frac{\Gamma}{H} \rho$, $\tilde{C}_r = \tilde{a}^4 \frac{\Gamma}{H} \tilde{\rho}$, which can be solved numerically for physically acceptable solutions: the resulting $a(t)$ and $\rho(t)$ of Fig. 1 show that our side density increases very sharply near $t=0$ because of the matter (and radiation) energy density variations produced by Γ while the scale factor is almost constant. The density reaches a maximum for $\Gamma/H = 3$ then decreases as expected according the actual equation of state of matter (here assumed in the plot to be that of cold matter with negligible pressure) as soon as the effect of Γ becomes negligible, insuring that in the present universe the variation of the gravitational coupling constant is completely out of reach to direct observation ($\frac{\Gamma}{H} \propto \frac{1}{a^4}$). This occurs when our side scale factor becomes dominant over $\tilde{a} = 1/a$. Eventually our cosmological equations were reconciled by the introduction of an additional degree of freedom, our scalar offshell (should not extremize the action) Γ . Notice that the conjugate densities are equal at the origin of time but also at the crossing time in Fig. 1. .

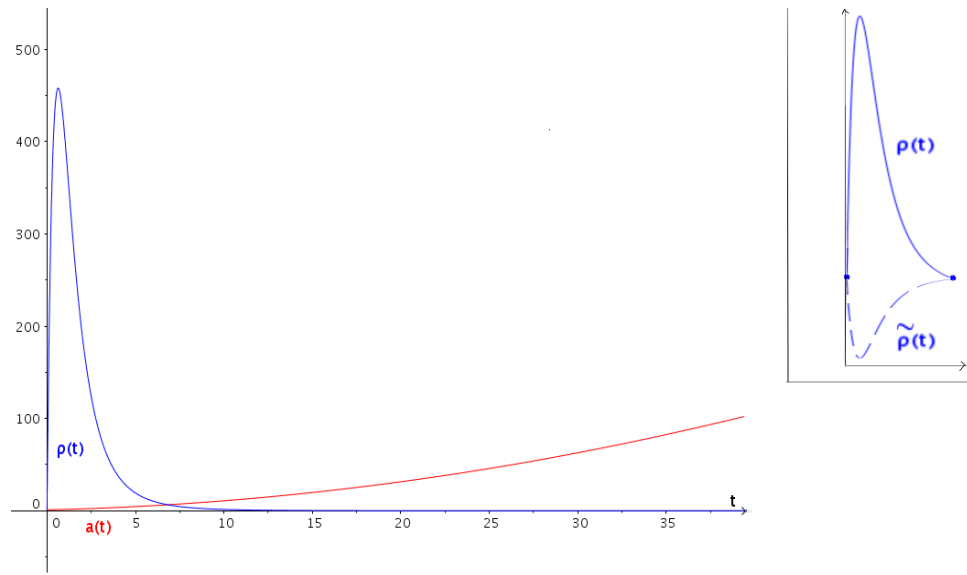


Fig. 1. $a(t)$ and $\rho(t)$ when including the effect of the transfer rate Γ to restore the consistency of Friedmann and conservation equations.

3. Cosmology

3.1. Reproducing GR cosmology

The expansion of our side implies that the dark side of the universe is in contraction. Provided dark side terms and the Γ terms can be neglected which is certainly an excellent approximation far from $t=0$, our cosmological equations reduce to

equations known to be also valid within GR. For this reason it is straightforward for DG to reproduce the same scale factor expansion evolution as obtained within the standard LCDM Model at least up to the redshift of its Lambda dominated era. The evolution of our side scale factor before the transition to the accelerated regime is depicted in red on the top left of Fig. 2 as a function of the conformal time t and the corresponding evolution laws as a function of standard time t' are also given in the radiative and cold era.

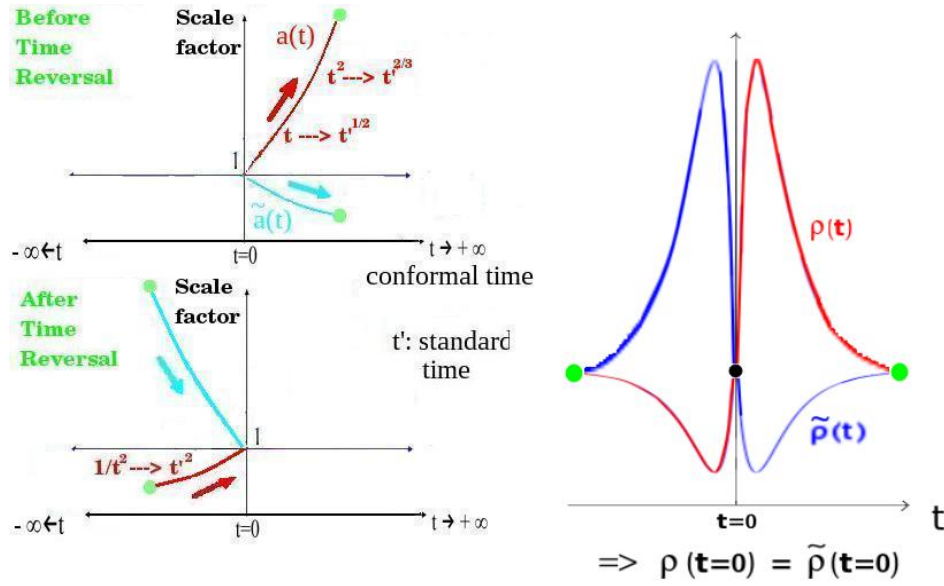


Fig. 2. Evolution laws and time reversal of the conjugate universes, our side in red

3.2. A discontinuous transition triggered the acceleration of the universe

The permutation symmetry of our equations (the two sides of the Janus field play the same role in them) allows a discrete transition to take place at the time the densities of the two sides cross each other : a permutation of the scale factor values keeping the densities and Hubble rates unchanged. This permutation (at the green point depicted on Fig. 2) could produce the subsequent recent acceleration of the universe. Specifically, just before the transition we have for instance: $a^4(\rho - 3p) \gg \tilde{a}^4(\tilde{\rho} - 3\tilde{p})$ just because $a(t) \gg \tilde{a}(t)$ and $\rho - 3p \approx \tilde{\rho} - 3\tilde{p}$ resulting in the usual (as in GR) expansion laws whereas just after the transition, $a^4(\rho - 3p) \ll \tilde{a}^4(\tilde{\rho} - 3\tilde{p})$ because now $a(t) \ll \tilde{a}(t)$ and $\rho - 3p \approx \tilde{\rho} - 3\tilde{p}$ resulting in the dark side source term now driving the evolution, producing a constant acceleration of our side scale factor in standard time coordinate t' following the transition redshift : $a(t') \propto t'^2$.

Because our solutions turn out to satisfy the fundamental relation:

$$\tilde{a}(t) = \frac{1}{a(t)} = a(-t) \quad (10)$$

we can also interpret our permutation symmetry as a global time reversal symmetry about privileged origin of conformal time $t=0$. Then the evolution of both densities and scale factors are cyclic as illustrated in Fig. 2. This also insures the stability of our homogeneous solutions in the sense that these remain bounded and confirms that we completely avoid any singularity issue. By the way having equal initial densities is also ideal to have equal amounts of matter and anti-matter at the origin of time, but then, following the separation of the two sides, a small excess of matter on our side corresponding to the same exact small excess of anti-matter on the conjugate side. This would presumably be the origin of the baryonic asymmetry of our universe after almost complete matter anti-matter annihilation.

Gravity from sources on our side is expected to be almost switched off at the transition. This problem can be solved for high density objects (stars, planet, DM clumps...) by considering spatial domains and discontinuities (see [1]) having far reaching consequences.

3.3. Confrontation with SN, BAO, CMB data

Let's stress that the following confrontation is more a proof of concept than a quantitative global statistical analysis as the latter would require all existing data to be reanalyzed with our theory as fiducial model to reevaluate all values and systematical errors and re correct for non linear effects. This challenging program (requiring a complete understanding of the evolution of fluctuations) is left for future work: to pave the way for it we here would like to more modestly try to avoid as much as possible doing combinations and rather want to isolate each observable (CMB, BAO, SN) to identify which kind of systematics could be at play for each. We believe this can also provide valuable insights for other kind of models such as IDE for which modeling the evolution of fluctuations is also very challenging. In this section t and H now denote the standard time and Hubble rate.

3.3.1. JLA and Pantheon SN

First noticeable is the remarkable (and not expected within LCDM) agreement between the supernovae Hubble diagram up to $z=0.6$ and a constantly accelerated universe [2] .ie. with $a(t) \propto t^2$ meaning a deceleration parameter $q=-0.5$. With the JLA sample of SN we fit α of a power law t^α evolution of the scale factor for redshifts restrained to the $[0, z_{\max}]$ interval to confirm this: $\alpha = 1.85 \pm 0.15$ for $z_{\max}=0.6$ (one standard deviation from 2.)

The parameter which replaces the cosmological constant in our framework is merely the redshift of densities equality i.e. the transition redshift z_{tr} . The next step is therefore to fit the transition redshift between a fixed $t^{2/3}$ and subsequent

t^2 evolution laws for the JLA SN sample, and we get: $z_{tr} = 0.67 + 0.24 - 0.12$ with a $\chi^2 = 740.8$ only slightly larger than that of the LCDM fit (739.4). We noticed a large shift of our fitted z_{tr} to a much smaller value on the Pantheon data, which was unexpected because most (3/4) supernovae were in common with JLA. We found that a recalibration of the lowest and highest z SNs was responsible for the shift and it was not clear which calibration was faulty so that hopefully only a future survey might clarify the situation. This, all the more since a pathologically looking two sigma wiggle appeared in the reconstructed $H(z)$ from those SN apparently just as a result of this new calibration (See Fig 1 of¹⁹ and Fig 2 of²⁰). Such wiggle was absent in the JLA LCDM best fit residuals: see Fig. 3.

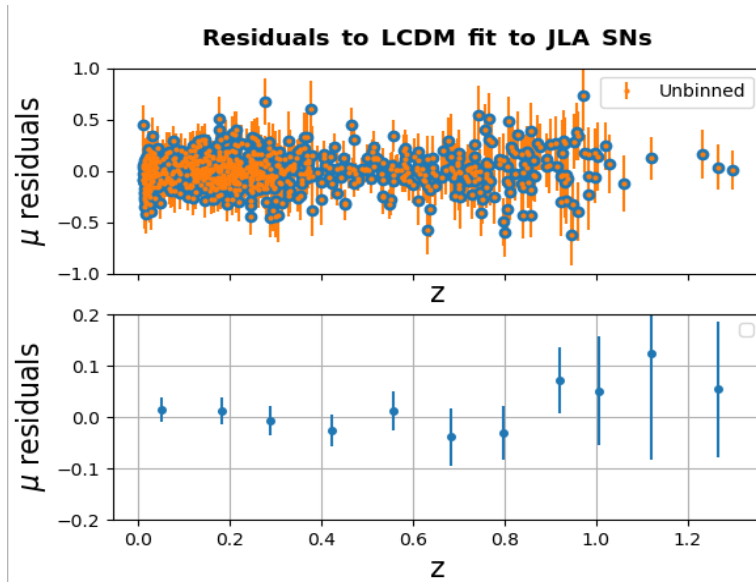


Fig. 3. Residuals to LCDM best fit to JLA data

We shall see what DESy5 has to say about this later.

3.3.2. CMB

The next step was to use our Geogebra interactive graphical tool to play with cursors and hopefully determine a z_{tr} value lying in the allowed interval according our previous SN fits, a H_0 close to the directly obtained value by Riess *et al.*^[3] (local distance ladder method through Cepheids and nearby SNs) and simultaneously allowing a good agreement to both the CMB data (angular position of first acoustic peak θ^* at decoupling and comoving sound horizon r_{drag})^[5] and BAO data ($H(z)$, $D_M(z)$)^[4].

At this level it already turned out that our $H(z)$ was several percent too large at

high z so that the fit of Planck data was doomed to failure (Fig. 4). An additional correction was therefore needed near the transition redshift. Several mechanisms have been considered to produce the Ad hoc correction (some of them very well physically motivated) of Fig. 5 that will be used throughout the article. However, following the recent discovery of a still not physically elucidated CMB new foreground that significantly cools down the temperature (≈ 15 microKelvin) in the direction of nearby spiral galaxy halos¹⁷, a foreground that remarkably correlates with the longstanding issue of the large scale anomalies of the CMB¹⁸, it is not excluded that the Planck cosmological parameters are in error, particularly if the new foreground is not negligible on scales related to the eISW effect. If for instance the density of matter ω_M has been underestimated by Planck because of this foreground then hopefully no correction is actually needed for DG. At the same time a several percent greater matter density would be helpful to explain most of the recently discovered JWST anomalies while subtracting the new foreground should also imply less power on the CMB largest scales probably meaning that LCDM overestimates the Late ISW effect which then favours most alternatives (including DG) that predict less Late ISW. The new unexpected foreground is challenging all so far considered mechanisms to explain it. As it is frequency independent, we are encouraged to suspect an exotic gravitational effect along the line of sight. However lensing effects or any effect deviating optical rays would not produce a systematic drop of temperature but rather a smoothing of the fluctuations on the corresponding scales. So it appears that we have to deal with a kind of new gravitational effect able to absorb part of the photons irrespective of their frequencies. This really looks like a confirmation of the ability of photons within DG to transit between the two sides of the universe anywhere the local potential vanishes (because there the conjugate metrics are equivalent from the point of view of photons) and the regions surrounding small scale density fluctuations such as galaxies are naturally where we expect to find these vanishing potentials more often.

Anyway, with our current ad hoc correction, meant to keep our expansion history asymptotically Planck best fit LCDM 2018 like, we insure that our r_{drag} is also the same. Ω_{rad} is fixed as usual from the present day photon and neutrino densities. What's new is that Ω_M is then not anymore a free parameter. Indeed, we may define $\Omega_M(z_{\text{tr}}) = \frac{8\pi G \rho_M(z_{\text{tr}})}{3H_{\text{tr}}^2} = 1 - \Omega_r(z_{\text{tr}}) \approx 1$ since, beyond the transition redshift, we are indistinguishable from a mere CDM flat cosmology without any dark energy nor cosmological constant. We can then extrapolate this to the usual present $\Omega_M = \frac{8\pi G \rho_M(0)}{3H_0^2}$ given that $\rho_M(z_{\text{tr}}) = \rho_M(0)(1 + z_{\text{tr}})^3$ and $H_{\text{tr}} = H_0(1 + z_{\text{tr}})^{1/2}$ for a constantly accelerated regime between $z=0$ and $z=z_{\text{tr}}$. Then, $\Omega_M = (1 + z_{\text{tr}})^{-2}$ but this parameter is not anymore useful as this matter is not anymore gravific after the transition redshift.

Our attempts resulted in one of the best fits for $z_{\text{tr}} = 0.68$ (see Fig. 5). Unsurprisingly (the theory now being asymptotically LCDM and our transition redshift tuned to get the same angular diameter distance to the CMB), the resulting

TT+TE+EE power spectra fit (obtained thanks to a Class code [10] suitably modified for our needs) $\Delta\chi^2$ is only +4.4 relative to LCDM. Only the very large scale TT and $\phi\phi$ power spectra are significantly sensitive to the effect of density fluctuations at redshifts lower than z_{tr} and since at such redshifts much work remains to be done to properly simulate the highly non trivial interactions between our and the dark side fluctuations at various scales, a simplified first step methodology was adopted consisting in the assumption of a homogeneous dark energy fluid that would produce the same $H(z)$ as DG in the accelerated universe. For this reason the TT and $\phi\phi$ power spectra obtained on the largest scales should only be considered as indicative of what we can expect from such naive assumption.

The confrontation with Big Bang nucleosynthesis data is also granted to be successful given how close to the LCDM one is our $H(z)$ at high redshift (Fig. 5) and now the confrontation to Planck and Lyman alpha data is also satisfactory (Fig. 6, 7).

3.3.3. BAO

Before DESI, only one BAO LoS point at 0.7 was apparently too high (see Fig. 5) for DG, the likely origin of this tension being that perturbations from the contracting dark side start to grow differently than within LCDM after the transition redshift and as their gravity dominates over our side dark matter gravity, those may deform the BAO peak in an unexpected way for those who analyze the data with LCDM as fiducial model to estimate various systematics.

There is actually no apparent tension for the pink points (Fig. 5) corresponding to the full shape analysis (in particular one should not compare measured values to the tip of the red curve at $z=0.7$ but to the average of the curve over a large 0.2 redshift bin). The only tension is for $H(z = 0.7)$ for the BAO peak only (white points) analysis method. The values are obtained through techniques [6] [7] [4], correcting various non-linear effects and reducing the errors in a highly fiducial model dependent way, for instance by modeling biases and redshift space distortions (RSD) in a way which is valid for LCDM but certainly not for Dark Gravity (there are several effects related to a wrong fiducial model choice: the conversion from redshift space to real space coordinates, reconstruction, the fitting template and RSD corrections). It is clear that a deviation of ± 0.1 in the CPL w_a parameter to estimate fiducial model related systematics in SDSS BAO points (or even ± 0.5 for DESI points) much underestimates the systematics now that the thawing dark energy trend observed in combination of observables do not exclude w_a as low as -3!

We notice that recent alternative analysis indeed advocate the use of the linear point in between the peak and the deep of the BAO [8] claiming it to be more robust to non linear effects and that being purely geometric, it can be extracted without a template relying on the assumption of a fiducial model, while the BAO peak only method uncertainties are underestimated by roughly a factor two. This

would likely explain why the full shape method obviously including both the peak and the deep, and therefore likely sharing some of the good properties of the linear point, is not in tension with DG.

An alternative, as fiducial model independent as possible, 2D method [9] trying to avoid any correlation with the longitudinal BAO more subject to fiducial model related uncertainties, was developed in the same spirit. The line of sight BAO information is completely given up in this approach and the transverse BAO scale is extracted by directly fitting the angular correlation function in thin redshift slices (to drastically reduce systematics related to projection effects), which leads to significantly larger (≈ 5 percent!) BAO angles that would make the H_0 tension even easier to alleviate (see yellow points in Fig. 5).

Including the recent DESI BAO¹⁶ points (in blue) confirms that there is something wrong with the BAO peak only method points which deviate not only from DG but also from LCDM in a very unexpected way at $z=0.5$ and 0.7 just apparently to help people realize that.

It is important to realize that the high H_0 value from direct measurements implies that $H(z)$ must be well above the LCDM $H(z)$ below redshift 0.5 and therefore much below in the redshift range $[0.5,1]$ to exactly compensate in the integral that gives the angular diameter distance to the CMB which is mandatory to fit the CMB first peak angle θ^* . Then we can notice that all problematic BAO points are at low z where the fiducial model choice (wa too close to 0) can be very misleading as this is where our DG deviates more drastically from LCDM, not only for los BAO but then also BAO transverse thanks to the 40% correlation between the two.

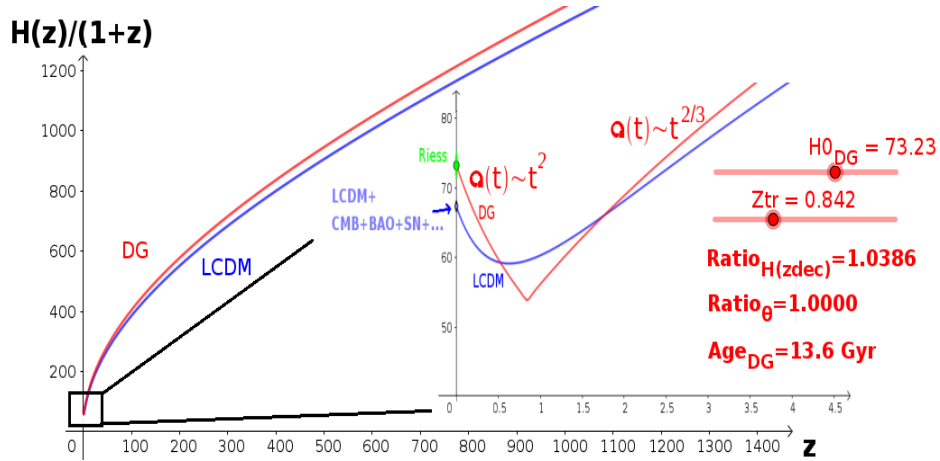


Fig. 4. A transition scenario vs the LCDM best fit

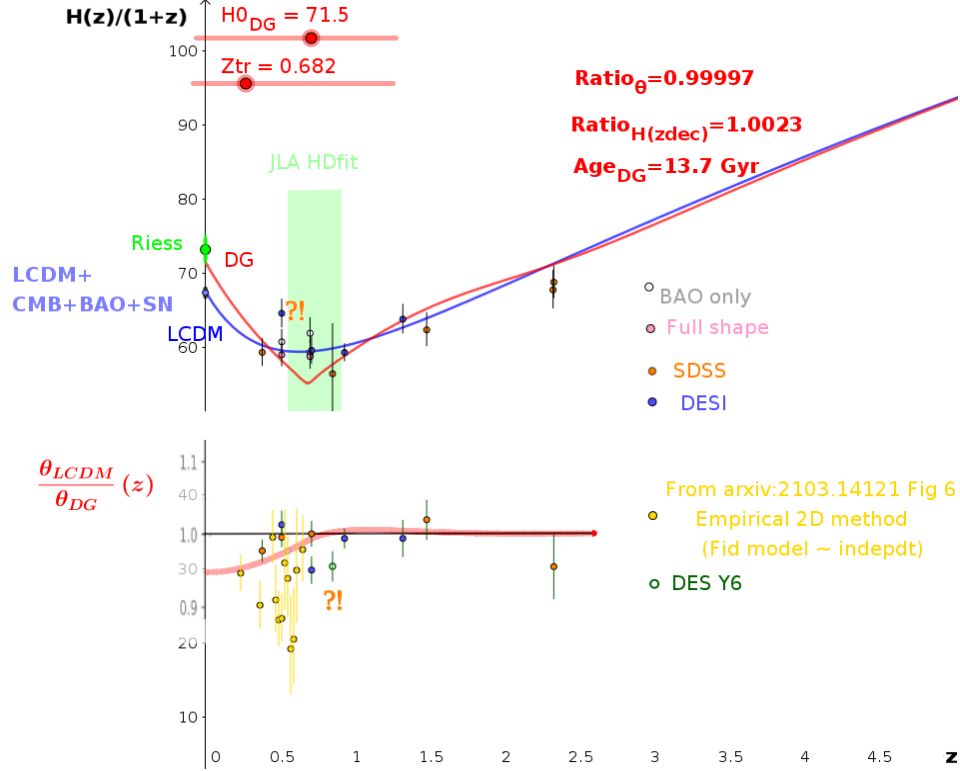


Fig. 5. A transition scenario confronted to Planck constraint on $H(z_{dec})$, and BAO data, the red curve is our prediction for $D_M(z)$ (bottom). The green band is the allowed interval for the transition redshift (within 1 standard deviation) according our SN Hubble diagram fit. In yellow are reported measurements using a less fiducial model dependent 2D method.

3.3.4. DESy5 SN

With the DESy5 SN data, we for the first time can explore the Hubble Diagram without having to rely on many intercalibration techniques of combined surveys (17 in Pantheon+ !) and many different selection bias corrections at the sensitivity limit of each survey! In particular we now have a golden redshift range $0.1 \leq z \leq 0.4$ where selection biases are almost negligible which is safer if we are not completely sure to understand how to accurately correct such biases. Of course significant bias corrections remain important in the shallow DES survey beyond 0.4 and in the deep survey beyond 0.7 as well as in the Low z Cfa/Csp survey used in combination, and understanding the intercalibration between DES ($z \geq 0.1$) and Cfa/Csp ($z \leq 0.1$) remains a critical issue. In Fig. 8 we have DESy5 residuals along with the best fitting curves of the CPL model to Pantheon+ in blue, to DESy5 in green and our DG model used as a reference as we consider that any natural (not fine tuned to produce a steep rise of $H(z)$ at very low z for instance) model successfully alleviating the $H0$ tension should be close to this one. Here the shapes rather than the rather

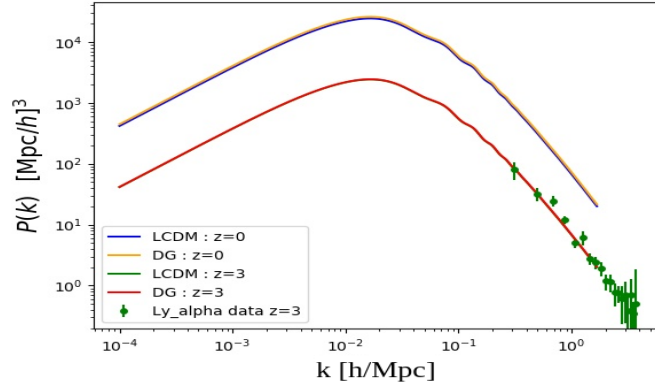


Fig. 6. DG confronted with Lyman-alpha (at mean $z=3$) Matter Power spectra and LCDM predicted Power spectra at $z=0$ and $z=3$

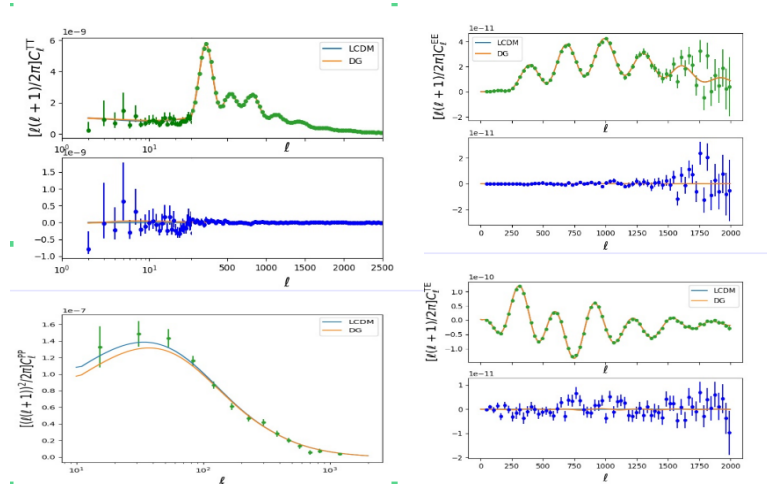


Fig. 7. DG confronted with Planck data and LCDM predicted Power spectra

arbitrary normalizations should be compared. We see that the tension between DG and Pantheon+ seems to be almost halfway reduced between DG and DESy5 and that the remaining tension is crucially depending on the Cfa/Csp vs DES intercalibration and our ability to correct biases at very large redshifts. As for the first issue we may wait for ZTF to clarify the situation as we remember that the lowz survey we are talking about is also one for which we have noticed very large discrepancies for the raw magnitudes (before standardization) between the past calibration methods (between JLA and Pantheon for instance). For the second issue

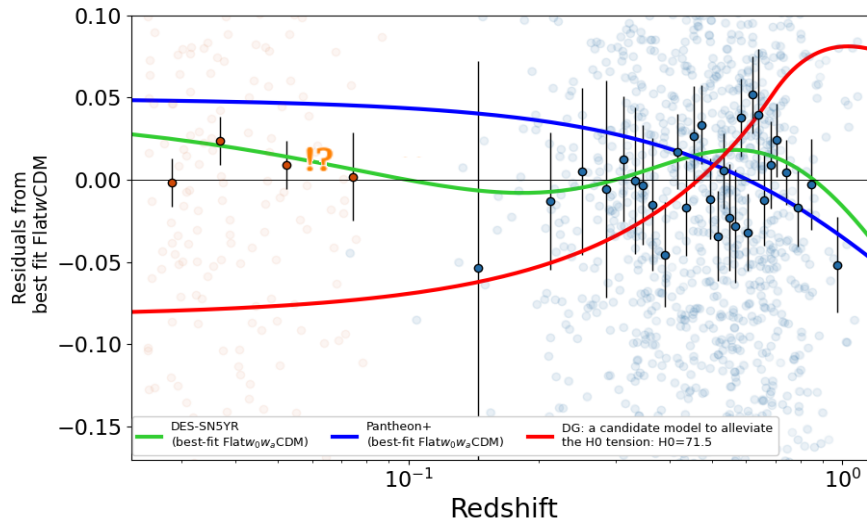


Fig. 8. DESy5 residuals and CPL best fits

it is reasonable to anticipate that as the golden redshift range extends to higher z in future surveys, the same that occurred between Pantheon+ and DESy5 in the golden redshift range will be confirmed at higher redshifts and we will get closer and closer to a thawing dark energy signal that mimics DG over an extended range of z instead of the currently restricted golden range. Indeed it is probably more fair to suspect the absence of thawing DE signal in Pantheon+ to be related to systematics than to suspect the presence of this signal in DESy5 to be produced by new systematics as many sources of systematics have obviously been eliminated and not introduced between the two. It remains that further reducing residual systematics in DESy5 is necessary to completely fill the gap with DG and a strong case for such remaining systematics is the 2 sigma tension between DESy5 and Planck (compare two sigma contours in Fig. 8 of¹⁵). Another is the low z pathological behaviour of DESy5 CPL best fit (!?) which alone speaks for highly underestimated intercalibration systematics between DES and Cfa/Csp.

3.4. S8 tension

Eventually, as for the S8 tension, our theory is in the same situation as many IDE models that also remarkably solve the Hubble tension with an even better global fit than Λ CDM if we take care to keep only BAO transverse data estimated by a model independent 2D method^[11]. According ^[11]: *'the S8 value estimated by weak lensing and galaxy clustering surveys data should be compared with the one estimated by the other data (such as Planck) assuming the same underlying*

model. Furthermore, it is important to mention that the accurate modeling of IDE framework on weak lensing and galaxy clustering data, especially with regard to the dynamics on non-linear scales and its application on the related observables, has not yet been addressed in the literature. Therefore, more conclusive findings cannot be made regarding the $S8$ tension in this class of IDE models’. It remains that in IDE models in which, relative to Λ CDM, DM dominates for a longer time and then transits much faster to the Dark Energy dominated era, one both expect an excess of lensing and clustering before the transition redshift followed by a significant decay of lensing and clustering variables after the transition redshift, a trend which seems to be already observed^[14]. Our theory belongs to this class of models as it can superficially be considered as a special kind of IDE model with a sudden transition (total decay) between dark matter and dark energy fluid with $w=-2/3$.

4. Conclusions

In contrast to a cosmological constant which just corresponds to one theoretical possibility out of a myriad of other terms that one could arbitrarily add either on the left or the right of the Einstein equation, everything in our framework follows from a different conceptual choice from the beginning: the existence of a non dynamical background. Our ability to solve the H_0 tension at the price of small tensions with the line of sight BAO points obtained by the peak only method is therefore remarkable given that systematical effects related to too wrong choices as for the fiducial model in their analysis could remove such residual tensions in our case. The ability to get a good fit to the SN HD diagram depends on the considered survey: perfect with JLA, very bad with Pantheon+, and now somewhat indecisive in DESY5. Future surveys both at low z and high z will hopefully clarify the situation.

DG is not merely a model but really a theoretical program with strong initial theoretical motivations and hopes that were not disappointed: it avoids singularity issues (both BH and primordial ones), explains the flatness of our universe, and is the ideal framework to understand the origin of the baryonic asymmetry and solve in the most simple way the old cosmological constant problem (see details in ^[1]).

References

1. Henry-Couannier, F. www.darksideofgravity.com/DG.pdf
2. F. Henry-couannier, C. Tao, A. Tilquin, Negative Energies and a Constantly Accelerating Flat Universe [arXiv:gr-qc/0507065](https://arxiv.org/abs/gr-qc/0507065)
3. A.G.Riess, A 2.4 percent Determination of the Local Value of the Hubble Constant,[arXiv:1604.01424](https://arxiv.org/abs/1604.01424)
4. S.Alam et al, The Completed SDSS-IV extended Baryon Oscillation Spectroscopic Survey: Cosmological Implications... [arXiv:2007.08991](https://arxiv.org/abs/2007.08991)
5. Planck collaboration, Planck 2018 results. VI. Cosmological parameters [arXiv:1807.06209](https://arxiv.org/abs/1807.06209)

6. Improving Cosmological Distance Measurements by Reconstruction of the Baryon Acoustic Peak D. J. Eisenstein , H-j Seo, E. Sirko , D. Spergel arXiv: astro-ph / 0604362
7. N. Padmanabhan, M. White, J.D. Cohn Reconstructing Baryon Oscillations: A Lagrangian Theory Perspective arXiv:0812.2905
8. arxiv:1811.12312 arxiv:1711.09063 arxiv:1703.01275 arxiv:1508.01170
9. E. de Carvalho, A. Bernui, F. Avila, C. P. Novaes, J. P. Nogueira-Cavalcante, 2021, BAO angular scale at $z_{\text{eff}} = 0.11$ with the SDSS blue galaxies, Astronomy and Astrophysics arxiv:2103.14121
10. D. Blas, J. Lesgourgues, T. Tram, 2011, The Cosmic Linear Anisotropy Solving System (CLASS) II: Approximation schemes, JCAP arxiv:1104.2933
11. A. Bernui, E Di Valentino, W. Giare, S Kumar, and R. C. Nunes Exploring the H_0 tension and the evidence of dark sector interaction from 2D BAO measurements arxiv:2301.06097
12. arXiv:1903.01823 Does gravity have to be quantized? Lessons from non-relativistic toy models. Antoine Tilloy
13. arXiv:0802.1978 Measurement Analysis and Quantum Gravity Mark Albers, Claus Kiefer, Marcel Reginatto
14. The growth of density perturbations in the last ≈ 10 billion years from tomographic large-scale structure data, Carlos Garcia-Garcia et al, arXiv:2105.12108 Fig. 8
15. DES Collaboration, The Dark Energy Survey: Cosmology Results With 1500 New High-redshift Type Ia Supernovae Using The Full 5-year Dataset arXiv:2401.02929
16. DESI Collaboration. DESI 2024 III: Baryon Acoustic Oscillations from Galaxies and Quasars arXiv:2404.03000
17. H E. Luparello, E F. Boero, M Lares, A G. Sánchez, D G Lambas The cosmic shallows I: interaction of CMB photons in extended galaxy halos arXiv:2206.14217
18. F K. Hansen, E F. Boero, H E. Luparello, D G Lambas A possible common explanation for several cosmic microwave background (CMB) anomalies: A strong impact of nearby galaxies on observed large-scale CMB fluctuations. ArXiv:2305.00268
19. Evolution of dark energy reconstructed from the latest observations Y Wang, L Pogosian, G Zhao and A Zucca2 arxiv:1807.03772
20. A. Riess et al Type Ia supernova distances at redshift greater than 1.5 from the Hubble Space Telescope multi-cycle treasury programs: the early expansion rate. arxiv:1710.00844